THE JOURNAL OF BIOLOGICAL CHEMISTRY VOL. 290, NO. 33, pp. 20086–20097, August 14, 2015

Lipid-induced Muscle Insulin Resistance Is Mediated by GGPPS via Modulation of the RhoA/Rho Kinase Signaling Pathway*

Received for publication, April 13, 2015, and in revised form, June 23, 2015 Published, JBC Papers in Press, June 25, 2015, DOI 10.1074/jbc.M115.657742

Weiwei Tao, Jing Wu, Bing-Xian Xie, Yuan-Yuan Zhao, Ning Shen, Shan Jiang, Xiu-Xing Wang, Na Xu, Chen Jiang, Shuai Chen, Xiang Gao, Bin Xue[1], and Chao-Jun Li[2]

From the Ministry of Education Key Laboratory of Model Animals for Disease Study, Model Animal Research Center and the School of Medicine, Nanjing University, Nanjing 210061, China

Background: GGPPS is overexpressed in the muscle of *ob/ob* mice, but its function remains unknown.
Results: Heterozygous knock-out of *GGPPS* in the skeletal muscle improved systemic insulin sensitivity and inhibited lipid-induced insulin resistance by decreasing RhoA/Rho kinase signaling.
Conclusion: GGPPS promotes lipid-induced muscle insulin resistance by enhancing RhoA/Rho kinase signaling.
Significance: GGPPS/RhoA/Rho kinase/IRS-1 axis is a novel pathway for the regulation of muscle insulin resistance.

Elevated circulating free fatty acid levels are important contributors to insulin resistance in the muscle and liver, but the underlying mechanisms require further elucidation. Here, we show that geranylgeranyl diphosphate synthase 1 (GGPPS), which is a branch point enzyme in the mevalonic acid pathway, promotes lipid-induced muscle insulin resistance through activation of the RhoA/Rho kinase signaling pathway. We have found that metabolic perturbation would increase GGPPS expression in the skeletal muscles of *db/db* mice and high fat diet-fed mice. To address the metabolic effects of GGPPS activity in skeletal muscle, we generated mice with specific GGPPS deletions in their skeletal muscle tissue. Heterozygous knock-out of *GGPPS* in the skeletal muscle improved systemic insulin sensitivity and glucose homeostasis in mice fed both normal chow and high fat diets. These metabolic alterations were accompanied by activated PI3K/Akt signaling and enhanced glucose uptake in the skeletal muscle. Further investigation showed that the free fatty acid-stimulated GGPPS expression in the skeletal muscle was able to enhance the geranylgeranylation of RhoA, which further induced the inhibitory phosphorylation of IRS-1 (Ser-307) by increasing Rho kinase activity. These results implicate a crucial role of the GGPPS/RhoA/Rho kinase/IRS-1 pathway in skeletal muscle, in which it mediates lipid-induced systemic insulin resistance in obese mice. Therefore, skeletal muscle GGPPS may represent a potential pharmacological target for the prevention and treatment of obesity-related type 2 diabetes.

Obesity is a risk factor for the development of insulin resistance. The obesity-induced elevation of circulating lipids, such as triglycerides and FFAs,[3] have been implicated in the pathogenesis of peripheral insulin resistance (1). However, the underlying mechanisms of FFA-induced insulin resistance require further elucidation. In skeletal muscle, FFA accumulation has been demonstrated to decrease insulin sensitivity in myotubes and contribute to insulin resistance in metabolic syndrome (2). FFAs promote insulin resistance in muscle through the phosphorylation of critical components of the insulin pathway (3). Increased FFAs cause the intracellular accumulation of FFA-derived lipid intermediates, such as diacylglycerols, ceramides, and long chain acyl-CoAs, which may activate some serine kinases (such as JNK, PKC, and IKK), leading to inhibitory IRS serine phosphorylation, thereby inhibiting the Akt pathway and downstream events (4, 5).

GGPPS is a branch point enzyme in the mevalonate pathway that catalyzes the synthesis of geranylgeranyl diphosphate (GGPP) from a single condensation of farnesyl pyrophosphate and isopentenyl pyrophosphate. Both farnesyl pyrophosphate and GGPP are used for the prenylation (farnesylation or geranylgeranylation) of proteins at their carboxyl-terminal CAA*X* motif, such as Ras and RhoA (6). GGPPS has been suggested to be involved in the regulation of pulmonary inflammation, osteoblast differentiation, male sterility, and heart failure (7–10). Previous studies in our laboratory have shown that GGPPS expression is elevated in insulin-resistant adipose tissues, which can lead to activation of the MAPK/Erk1/2 pathway through Ras prenylation, which is responsible for the inhibition of insulin signaling (11, 12). Previous studies have also demonstrated that GGPPS is overexpressed in the fat and skeletal muscle tissues of *ob/ob* mice (13). Thus, we hypothesized that overexpression of muscle GGPPS induced by an overabundance of

* This work was supported by Chinese National Program on Key Basic Research Project 973 Grant 2012CB524900 (to C.-J. L.), by National Natural Science Foundation of China Grant 31171306, and by Nature Science Foundation of Jiangsu Province Grant BK2011568 (to B. X.). The authors declare that they have no conflicts of interest with the contents of this article.

[1] To whom correspondence may be addressed: Model Animal Research Center and the School of Medicine, Nanjing University, Nanjing 210061, China. Tel. and Fax: 86-25-83596289; E-mail: xuebin@nju.edu.cn.
[2] To whom correspondence may be addressed: Model Animal Research Center and the School of Medicine, Nanjing University, Nanjing 210061, China. Tel. and Fax: 86-25-83596289; E-mail: licj@nju.edu.cn.

[3] The abbreviations used are: FFA, free fatty acid; GGPPS, geranylgeranyl diphosphate synthase 1; GGPP, geranylgeranyl diphosphate; GGTI, geranylgeranyltransferase I inhibitor; HFD, high fat diets; GTT, glucose tolerance tests; ITT, insulin tolerance tests; qRT-PCR, quantitative RT-PCR.

FFAs in obese individuals may contribute to the pathogenesis of muscle insulin resistance in type 2 diabetes.

To address the effects of muscle GGPPS on insulin resistance and glucose homeostasis, we generated muscle-specific *GGPPS* knock-out mice with the deletion of GGPPS in their postnatal skeletal muscles. Our data demonstrate that GGPPS-controlled protein geranylgeranylation mediates lipid-induced skeletal muscle insulin resistance by enhancing RhoA/Rho kinase signaling, suggesting that skeletal muscle GGPPS may represent a potential pharmacological target for the treatment of insulin resistance and type 2 diabetes.

Experimental Procedures

Reagents and Antibodies—GGPP, geranylgeranyltransferase I inhibitor (GGTI), and palmitate were purchased from Sigma-Aldrich. Fasudil was purchased from Cayman Chemical. The anti-RhoA, anti-GGPPS, anti-Rock1, and anti-Rock2 antibodies were purchased from Santa Cruz Biotechnology, the anti-α-tubulin antibody was obtained from Bioworld Technology, the anti-prenyl antibody was purchased from Abcam, the anti-IRS-1 (Tyr) antibody was purchased from Upstate, and the anti-p-Erk1/2, anti-Erk1/2, anti-p-Akt (Ser473), anti-Akt, anti-p-IR (Tyr1150/1151), anti-IR, anti-IRS-1 (Ser-307), anti-IRS-1 (Ser-632/5), and anti-IRS-1 antibodies were provided by Cell Signaling Technology.

Animals—We generated muscle-specific *GGPPS* knock-out mice by crossing MCK-Cre transgenic mice with homozygous floxed *GGPPS* mice. The generation of *GGPPS*-floxed mice has been previously described (7). The knock-out lines (strain 129) were backcrossed for a minimum of six generations to the C57BL/6 background, which was the background of the *GGPPS*-LoxP mice. All of the mice used in this study were males. For analysis of protein expression after insulin stimulation in muscle tissues, mice at 8 weeks of age were given an intraperitoneal injection of insulin (1 unit/kg of body weight) for 10 min. For high fat diet, mice at 6 weeks of age were maintained on a regular rodent chow or a high fat diet containing 60% fat-derived calories (Research Diets) for 12 weeks. The mice were housed under a 12-h light/12-h dark cycle in a temperature- and humidity-controlled environment and were fed *ad libitum*. All procedures followed in this investigation conformed to the approved regulations set forth by the Laboratory Animal Care Committee at Nanjing University.

Cell Culture and siRNA Transfection—Rat L6 myoblasts expressing c-MYC-GLUT4 were maintained in α-MEM containing 10% FBS at 37 °C in a humidified atmosphere with 5% CO_2. Once the myoblasts had grown to confluence in plates, the medium was replaced with α-MEM containing 2% fetal bovine serum to induce differentiation into myotubes. The cells were maintained for 6 days before the experiments were conducted, and the medium was changed every 48 h during this time. For siRNA transfection, L6-c-MYC-GLUT4 myotubes were incubated in antibiotic-free α-MEM, supplemented with 2% fetal bovine serum, and then transfected with siRNA of Scrb sequence or siRNA specific for GGPPS or RhoA, using Lipofectamine 2000 (Invitrogen) according to the manufacturer's protocols. siRNA sequences are shown in Table 1.

TABLE 1
List of PCR primers and siRNA sequences

Gene symbol	Primers
Cre	
Forward	5′-TGCCACGACCAAGTGACAGCAATG-3′
Reverse	5′-AGAGACGGAAATCCATCGCTCG-3′
Loxp	
Forward	5′-AATTGTGTGTGGTAGGGGTA-3′
Reverse	5′-AACTTGCTTCAGAACTGAGC-3′
GGPPS (mouse)	
Forward	5′-TTTTGCATACACTCGACACACT-3′
Reverse	5′-ACCACAGGCCTCAATTTGTTTGT-3′
Rock1 (mouse)	
Forward	5′-GACTGGGGACAGTTTTGAGAC-3′
Reverse	5′-GGGCATCCAATCCATCCAGC-3′
Rock2 (mouse)	
Forward	5′-TTGGTTCGTCATAAGGCATCAC-3′
Reverse	5′-TGTTGGCAAAGGCCATAATATCT-3′
36B4 (mouse)	
Forward	5′-GAAACTGCTGCCTCACATCCG-3′
Reverse	5′-GCTGGCACAGTGACCTCACACG-3′
Rock1 (rat)	
Forward	5′-CTGGGAAGAAAGGGACATCA-3′
Reverse	5′-TTCAGGCACATCGTAGTTGC-3′
Rock2 (rat)	
Forward	5′-CAGGGAGGTACGACTTGGAA-3′
Reverse	5′-ACATCGCCTTTGTCATCCTC-3′
18S (rat)	
Forward	5′-AAACGGCTACCACATCCAAG-3′
Reverse	5′-CCTCCAATGGATCCTCGTTA-3′
Scrb	
Forward	5′-UUCUCCGAACGUGUCACGU-3′
Reverse	5′- ACGUGACACGUUCGGAGAA-3′
GGPPS siRNA	
Forward	5′- UUCUCCGAACGUGUCACGU-3′
Reverse	5′-ACGUGACACGUUCGGAGAA-3′.
RhoA siRNA	
Forward	5′-CAGACACUGAUGUUAUACU-3′
Reverse	5′-AGUAUAACAUCAGUGUCUG-3′
Rock1 siRNA	
Forward	5′-UCCAAGUCACAAGCAGACAAGGAUU-3′
Reverse	5′-AAUCCUUGUCUGCUUGUGACUUGGA-3′
Rock2 siRNA	
Forward	5′-CCGGACCCAUGGAUCAGAGAUAAUU-3′
Reverse	5′-AAUUAUCUCUGAUCCAUGGGUCCGG-3′

mRNA and Protein Expression Analysis—Total RNA was isolated using TRIzol reagent (Invitrogen), reverse transcribed, and analyzed by quantitative PCR using SYBR Green and an ABI 7300 system (Applied Biosystems, Carlsbad, CA). Primers for 36B4 (mouse) or 18S (rat) were included for normalization. A complete list of PCR primers is shown in Table 1. For protein analysis, we directly lysed cells or homogenized tissues in an Nonidet P-40 lysis buffer and centrifuged for 10 min at 14,000 × *g* and 4 °C. The resulting supernatant fraction was separated by SDS-PAGE and immunoblotted with relative antibodies. For immunoprecipitation, lysates were immunoprecipitated with their corresponding antibodies and then with protein A/G coupled to agarose beads (Santa Cruz Biotechnology). After a thorough wash, the samples were eventually subjected to immunoblotting analysis. The intensities of the bands were quantified using National Institutes of Health ImageJ software. All the phosphorylated or prenylated proteins were normalized to each specific total protein. Other proteins were normalized to each loading control α-tubulin.

Prenylation and Membrane Association Measurements—To test the prenylation of RhoA, we directly lysed cells or homog-

enized tissues in an Nonidet P-40 lysis buffer and centrifuged for 10 min at 14,000 × *g* and 4 °C. The supernatant fractions were immunoprecipitated with the anti-RhoA antibody (Santa Cruz Biotechnology). After a thorough wash, the samples were eventually subjected to immunoblotting analysis using the anti-prenyl antibody (Abcam). To determine the membrane association of RhoA, subcellular fractionation was performed using ultracentrifugation as previously described (14). In brief, the cell pellets or tissues were lysed and homogenized with ice-cold Dounce tissue homogenizer, and the lysates were centrifuged at 100,000 × *g* for 30 min (4 °C). The supernatant represents the cytosolic fraction, and the pellet represents the membrane fraction. All of the aforementioned samples were subjected to immunoblotting analysis using the anti-RhoA antibody.

Glucose and Insulin Tolerance Tests (GTT and ITT)—To test glucose tolerance, mice were given an intraperitoneal injection of glucose (2 mg/g of body weight) after a 16-h fast. To determine insulin sensitivity, mice were given an intraperitoneal injection of insulin (1 unit/kg of body weight) after a 4-h fast. Blood glucose levels were determined at the indicated times from tail blood using the Accu-Check Glucometer (Roche Diagnostics).

Glucose Uptake—Measurement of glucose uptake in the cells was performed as previously described (15), with modifications. In brief, cells were washed three times with Hepes buffer and then stimulated with 100 nM insulin in Hepes buffer for 20 min. Next, they were incubated with 1 μCi of [^{3}H]2-deoxyglucose (PerkinElmer Life Sciences) and 0.1 mM of 2-deoxyglucose for 5 min. After incubation, the cells were washed three times with ice-cold PBS and dissolved in 1 N NaOH. The solution was neutralized with 1 N HCl, and the radiolabeled glucose in solution was counted by a liquid scintillation counter.

Muscle Incubation and Glucose Uptake ex Vivo—Soleus muscles were isolated and incubated with or without 10 milliunits/ml insulin in Krebs-Ringer bicarbonate buffer for 50 min as described previously (16). After incubation, the muscles were used for the glucose uptake assay as described previously (17). After glucose uptake, the muscles were snap frozen, weighed, and processed as described previously (17). Radioisotopes in the muscles were counted using a MicroBeta2 Plate Scintillation Counter (PerkinElmer Life Sciences).

Metabolic Parameters—Blood samples were obtained from the vena cava, and the plasma samples were stored at −80 °C until analysis. Glucose levels were determined using an Accu-Check Glucometer. Blood triglyceride, FFA, cholesterol, and muscle triglyceride concentrations were determined by enzymatic assays using commercial kits according to the manufacturer's protocols. Plasma insulin concentrations were measured using an ELISA kit from Millipore.

Histology—Tissues were dissected, frozen in isopentane that had been cooled in liquid nitrogen, and then embedded in OCT compound (Leica Microsystems, Heidelberg, Germany) and sectioned. HE staining was performed according to standard procedures by histology. Skeletal muscle fiber type (I, IIa, and IIb) was quantified using myosin ATPase staining. Sections were subjected to acidic preincubation (0.2 M sodium acetate and 0.1 M KCl, pH 4.43), exposed to ATP (90 mM glycine, 65 mM $CaCl_2$, 90 mM NaCl, and 3 mM ATP, pH 9.4), and subsequently treated with 1% (w/v) $CaCl_2$, 2% (w/v) $CoCl_2$, and 1% (v/v) $(NH_4)_2S$. Following histological analysis, coverslips were secured over the slides with aqueous mounting medium. Images for fiber type analysis were captured using an Olympus DP71 camera (Olympus Corp., Tokyo, Japan) and Image-Pro Express software.

Treadmill Running—We performed treadmill running studies using a motorized, speed-controlled treadmill system (Columbus Instruments, Columbus, OH). Fed mice ran for 12 min at 9 m min^{-1} followed by an increase of 1 m min^{-1} every 6 min until exhaustion. A level inclination angle was used. The mice were trained at a speed of 9 m min^{-1} for 5 min for three sessions to acquire running skills prior to the tests.

Rotarod Test—Mice were placed on a rod of a rotarod (IITC Life Science, Woodland Hills, CA) rotating at an initial speed of 1 rpm, which was quickly increased to 20 rpm, and the time that the mice stayed on the rod was recorded. The mice were trained at a speed of 20 rpm for 5 min for 3 days to acquire running skills before the rotarod tests.

Statistical Analysis—The data are presented as the means ± S.D. We performed statistical comparisons with an unpaired two-tailed Student's t test. $p < 0.05$ was considered statistically significant.

Results

GGPPS Expression Is Enhanced in the Skeletal Muscle Tissue of Mice with Obesity-related Diabetes—We found that GGPPS expression was enhanced both at the mRNA and protein levels in the gastrocnemius muscle tissue of obese diabetic *db/db* mice and HFD-induced obese mice (Fig. 1, *A* and *B*). This phenomenon was further confirmed at the cellular level. Following the treatment of L6 myotubes with the palmitate, GGPPS expression was also enhanced (Fig. 1*C*). However, insulin itself had no effect on GGPPS expression (Fig. 1*D*). These data suggest that metabolic perturbation caused by FFA elevations may alter GGPPS expression in skeletal muscle tissue.

To assess whether elevated GGPPS in the skeletal muscle of obese mice contributes to the development of insulin resistance, we generated muscle-specific *GGPPS* knock-out mice (MCK-*GGPPS*$^{-/-}$) by breeding animals harboring a floxed *GGPPS* allele with mice that transgenically expressed Cre recombinase under the control of the MCK promoter (Fig. 2*A*). The deletion of *GGPPS* drastically reduced GGPPS expression in the gastrocnemius and soleus muscles of MCK-*GGPPS*$^{-/-}$ and MCK-*GGPPS*$^{+/-}$ mice (Fig. 2, *B–D*). Because MCK is also expressed in *cardiac* muscle tissues, the MCK-Cre-driven *GGPPS* deletion also resulted in a decrease in GGPPS expression in cardiomyocytes (Fig. 2*D*). There were no significant weight differences in body, liver, epididymal fat pad, and muscles among the MCK-*GGPPS*$^{-/-}$, MCK-*GGPPS*$^{+/-}$, and MCK-*GGPPS*$^{+/+}$ mice, with the exception of heart weight, which was increased in the MCK-*GGPPS*$^{-/-}$ mice (Fig. 2*E*).

Heterozygous Knock-out of GGPPS in Skeletal Muscle Improves Systemic Insulin Sensitivity of Mice—We found that MCK-*GGPPS*$^{+/-}$ and MCK-*GGPPS*$^{-/-}$ mice showed significant improvements in glucose tolerance and insulin sensitivity by performing intraperitoneal GTT and ITT (Fig. 3*A*). The mutant mice showed lower blood glucose levels than that of

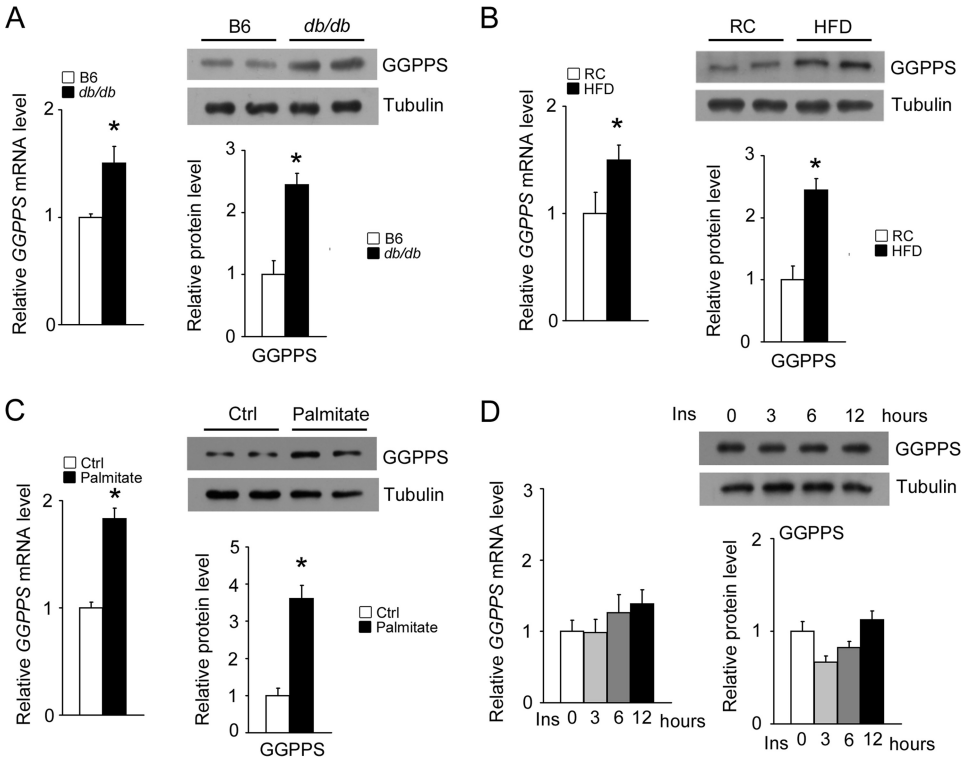

FIGURE 1. **Expression of GGPPS in skeletal muscle of insulin-resistant mice.** *A* and *B*, qRT-PCR and immunoblot analysis of GGPPS expression in the gastrocnemius muscles of wild-type and *db/db* mice at 8 weeks of age or B6 mice fed a regular chow diet or HFD for 12 weeks ($n = 5$). *C* and *D*, qRT-PCR and immunoblot analysis of GGPPS expression in L6 myotubes incubated with 0.75 mM palmitate for 16 h or 100 nM insulin for the indicated time points. The data represent means ± S.D. *, $p < 0.05$. *Ctrl*, control; *Ins*, insulin; *RC*, regular chow diet.

WT mice in the fed state (Fig. 3*B*). However, blood insulin levels did not significantly differ between the groups (Fig. 3*B*). Other metabolites, such as blood triglycerides, FFAs, and total cholesterol, also did not significantly differ (Fig. 3, *B* and *C*). Similar GTT and ITT results were observed in the homozygous and heterozygous mice; therefore, we only further examined the heterozygous mice because all homozygous mice died of heart hypertrophy at between 8 and 13 weeks of age (data not shown), which is consistent with our previous research (7).

To clarify whether these improvements were the result of augmented muscle glucose uptake, we first used isolated soleus muscle to perform a glucose uptake assay. Heterozygous knock-out of *GGPPS* in soleus muscle enhanced glucose uptake under both normal and insulin-stimulated conditions (Fig. 3*D*). Next, we also perform a glucose uptake assay in cultured L6 myotubes. Glucose uptake assessment showed that overexpression of GGPPS effectively reduced glucose uptake under normal conditions or insulin stimulation, whereas knockdown of GGPPS enhanced glucose uptake (Fig. 3*E*). The regulation of glucose uptake by GGPPS is dependent on protein geranylgeranylation because GGPP administration was able to decrease glucose uptake similar to what was observed following GGPPS overexpression, whereas the administration of the geranylgeranyltransferase I inhibitor GGTI was able to increase glucose uptake similar to what was observed following GGPPS knockdown (Fig. 3*F*). Thus, these results suggest that the heterozygous knock-out of *GGPPS* in skeletal muscle increased muscle glucose uptake and systemic insulin sensitivity.

We found that the properties of the skeletal muscle were not altered after *GGPPS* knock-out. Histochemical analysis of the tibialis anterior (TA) or soleus muscle revealed that there were no differences in muscle fiber morphology among the groups (Fig. 3*G*). The composition of the muscle fiber types was not altered by the GGPPS deletion (Fig. 3, *H* and *I*). The running ability of the MCK-*GGPPS*$^{+/-}$ mice was similar to that of the WT mice (Fig. 3*J*). The rotarod test also indicated no difference in exercise and balance capacity between the MCK-*GGPPS*$^{+/-}$ and control mice (Fig. 3*K*). Thus, we conclude that the metabolic improvement of skeletal muscle is not related to its properties or performance alteration.

Insulin Signaling Is Augmented by Heterozygous Knock-out of GGPPS in Skeletal Muscle—Because heterozygous knock-out of *GGPPS* in skeletal muscle increases glucose uptake and insulin sensitivity, we next assessed insulin pathway in skeletal muscle tissue and L6 myotubes. Notably, we found that the basal phosphorylation level of IRS-1 (Tyr) and Akt (Ser-473) was markedly enhanced, but IR (Tyr-1150/1151) and Erk1/2 phosphorylation was unaffected in the gastrocnemius muscle of MCK-*GGPPS*$^{+/-}$ mice (Fig. 4*A*). We also found IRS-1 (Ser-307) phosphorylation was reduced, whereas that of IRS-1 (Ser-632/635) was unaffected in the MCK-*GGPPS*$^{+/-}$ mice (Fig. 4*A*). Heterozygous knock-out of *GGPPS* further enhanced insulin-stimulated Akt activation but not Erk1/2 activation (Fig. 4*B*). These results suggest that GGPPS may control insulin signaling through regulating IRS-1 function. The examination of insulin signaling in L6 myotubes showed that GGPPS overexpression robustly reduced Akt phosphorylation and enhanced IRS-1 (Ser-307) phosphorylation, whereas its knockdown significantly enhanced Akt phosphorylation and decreased IRS-1 (Ser-307) phosphorylation (Fig. 4, *C* and *D*). The

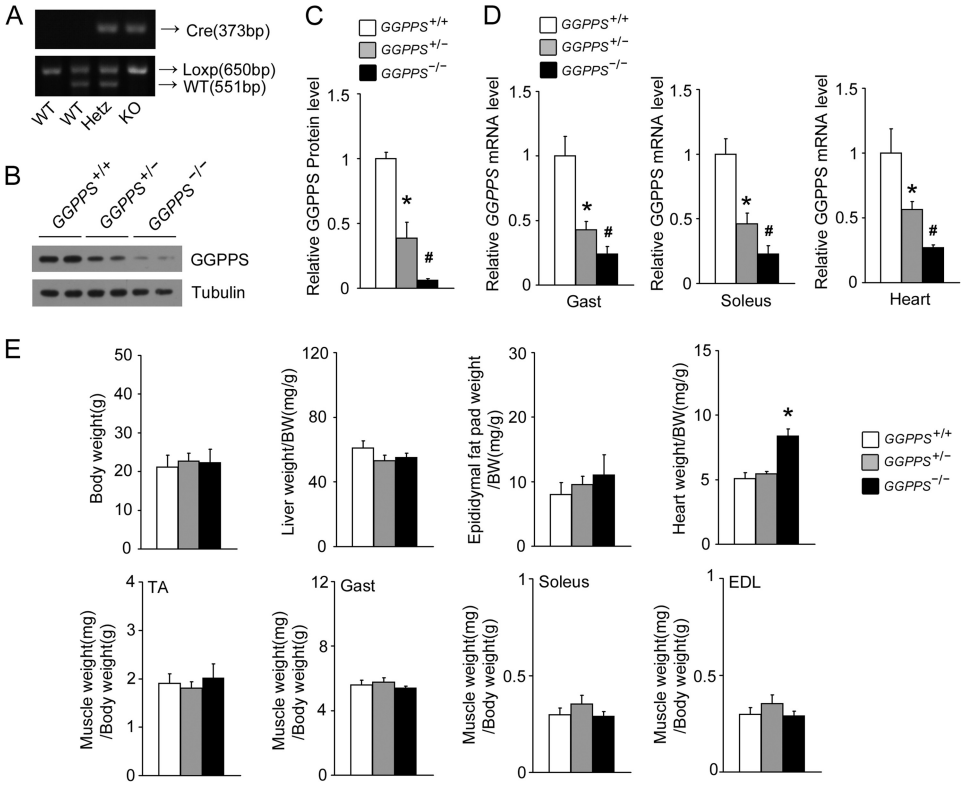

FIGURE 2. **Generation and characterization of muscle-specific *GGPPS*-deficient mice.** *A*, PCR genotyping of WT, heterozygous, and KO mice using primers of Cre and Loxp. The *upper gel* shows Cre genotyping, the PCR product is 373 bp. The *lower gel* shows *GGPPS* genotyping of the same animals. Tail DNA was amplified using Loxp primers, yielding products of 650 and 551 bp for the floxed and wild-type alleles, respectively. *B* and *C*, Western blot analysis of GGPPS protein in the gastrocnemius muscles of WT, MCK-*GGPPS*$^{+/-}$, and MCK-*GGPPS*$^{-/-}$ mice ($n = 4$). *D*, qRT-PCR analysis of GGPPS expression in the gastrocnemius muscles, soleus muscles, and hearts for the indicated genotypes ($n = 4$). *E*, body weight and multiple tissue weights of 8-week-old mice ($n = 5–6$). The data represent means ± S.D. * and #, $p < 0.03$ compared with the WT MCK-*GGPPS*$^{+/+}$ mice. *EDL*, extensor digitorum longus; *Gast*, gastrocnemius muscle; *Hetz*, heterozygous.

administration of GGPP or GGTI to L6 myotubes revealed that Akt and IRS-1 (Ser-307) phosphorylation was affected in a time-dependent manner (Fig. 4, *E–G*). These results suggest that GGPPS-controlled protein geranylgeranylation is able to regulate insulin signaling in skeletal muscle and L6 myotubes.

Geranylgeranylation of RhoA Is Responsible for GGPPS-regulated Insulin Signaling—Protein prenylation, including geranylgeranylation and farnesylation, is a critical process for the membrane association of many signaling proteins, including Ras and Ras-related small GTP-binding proteins, such as Rho, Rab, and Rac (6). As a geranylgeranylated protein, RhoA was reported to enhance the phosphorylation of IRS-1 (Ser-307 and Ser-632/635 residues) and impairs insulin signaling by activating Rho kinase (18–21). We indeed found IRS-1 (Ser-307) phosphorylation was reduced in the MCK-*GGPPS*$^{+/-}$ mice. Thus, we checked the prenylation of RhoA in the WT and MCK-*GGPPS*$^{+/-}$ mice. The present study showed that the membrane association and prenylation of RhoA were both decreased in the gastrocnemius muscle of MCK-*GGPPS*$^{+/-}$ mice (Fig. 5*A*). The membrane association (Fig. 5, *B* and *C*) and prenylation (Fig. 5, *D* and *E*) of RhoA were dependent on GGPPS, and these processes were significantly enhanced by GGPPS overexpression or GGPP treatment and reduced by GGPPS knockdown or GGTI treatment in the L6 myotubes.

To confirm that the GGPPS-regulated insulin pathway occurred directly through the action of RhoA, we knocked down RhoA using siRNA. As expected, the increased phosphorylation of IRS-1 (Ser-307) caused by GGPPS overexpression or GGPP administration was largely prevented by RhoA knockdown (Fig. 5*F*), which suggest that the GGPPS-regulated phosphorylation of IRS-1 (Ser-307) was dependent on RhoA. Because RhoA knockdown could also restore the decreased Akt phosphorylation (Fig. 5, *G* and *H*) and glucose uptake (Fig. 5*I*) by GGPPS overexpression or GGPP administration, we further confirm that RhoA is responsible for the regulation of insulin signaling by GGPPS in muscle cells. Collectively, our results confirm that RhoA geranylgeranylation is responsible for GGPPS-regulated insulin signaling and contributes to the development of muscle insulin resistance.

RhoA/Rho Kinase Pathway Mediates GGPPS-regulated Insulin Signaling—To confirm that GGPPS regulates the insulin pathway directly through RhoA/Rho kinase signaling, the Rho kinase inhibitor fasudil was used. Fasudil treatment notably inhibited the up-regulation of IRS-1 (Ser-307) phosphorylation induced by GGPPS overexpression or GGPP administration (Fig. 6*A*). Fasudil treatment also restored the decreased phosphorylation of Akt by GGPPS overexpression or GGPP administration (Fig. 6, *B* and *C*). The inhibition of glucose uptake by GGPPS or GGPP was also decreased following treatment with fasudil (Fig. 6*D*). Because both Rho kinase isoforms Rock1 and Rock2 are expressed in skeletal muscle tissues, we next examined which Rho kinase isoform mediated the regulation of insu-

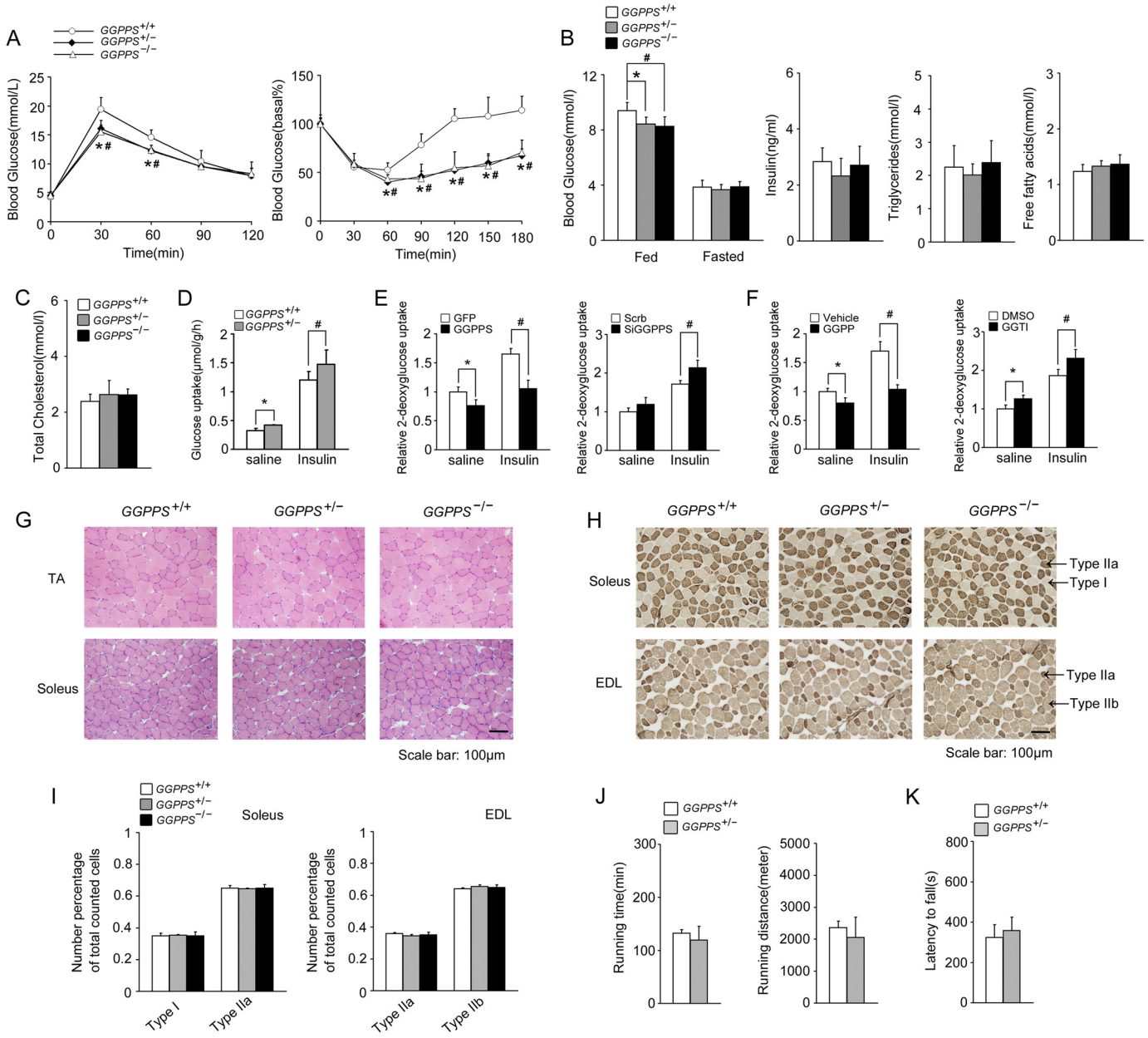

FIGURE 3. **Improved insulin sensitivity and glucose homeostasis in MCK-*GGPPS*$^{+/-}$ and MCK-*GGPPS*$^{-/-}$ mice.** *A–C*, GTTs, ITTs, blood glucose, fed insulin, fasted triglycerides, fasted FFAs, and fasted cholesterol levels in mice fed a chow diet ($n \geq 6$). *D*, glucose uptake in soleus muscle *ex vivo* ($n = 5–8$). *E*, glucose uptake in L6 myotubes infected with the GFP or GGPPS adenovirus or transfected with Scrb or GGPPS siRNA for 48 h. *F*, glucose uptake in L6 myotubes administered GGPP or GGTI for 12 h. *G*, cross-sections of the tibialis anterior and soleus muscles of mice stained with hematoxylin and eosin ($n = 5$). *H*, cross-section of the soleus and extensor digitorum longus muscles of mice stained for myo-ATPase. *I*, quantification of muscle fiber types in the soleus and extensor digitorum longus muscles based on myo-ATPase staining. *J*, running time and distance of mice subjected to endurance exercise on a motorized treadmill ($n = 6–7$). *K*, rotarod test for the indicated genotypes of mice ($n = 6–7$). All mice used were 8 weeks of age. The data are shown with means ± S.D. * and #, $p < 0.05$. *EDL*, extensor digitorum longus; *TA*, tibialis anterior.

lin pathway by GGPPS/RhoA signaling. First, we found that *Rock2* mRNA levels were higher than Rock1 in multiple muscle tissues and L6 myotubes (Fig. 6, *E* and *F*). This result suggests that Rock2 may mainly mediate the upstream GGPPS/RhoA signaling to regulate insulin pathway. Because knockdown of Rock2, but not Rock1, could restore the decreased Akt phosphorylation (Fig. 6*G*) and glucose uptake (Fig. 6*H*) by GGPPS overexpression, we demonstrate that Rock2 is responsible for the regulation of insulin signaling by GGPPS in muscle cells. These results confirm that GGPPS regulates the insulin pathway directly through the RhoA/Rho kinase signaling pathway.

Heterozygous Knock-out of GGPPS in Skeletal Muscle Protects Mice from HFD-induced Insulin Resistance—To further confirm that muscle GGPPS promotes lipid-induced insulin resistance, we also assessed the regulation of GGPPS on systemic insulin sensitivity using a lipid-induced insulin resistance model. GTT and ITT examination suggested that heterozygous knock-out of *GGPPS* significantly improved glucose tolerance and insulin sensitivity when mice were fed an HFD in the absence of changes in levels of insulin or other metabolic parameters (Fig. 7, *A–C*). Similar reactions of L6 myotubes were also observed in a palmitate treatment model, indicating

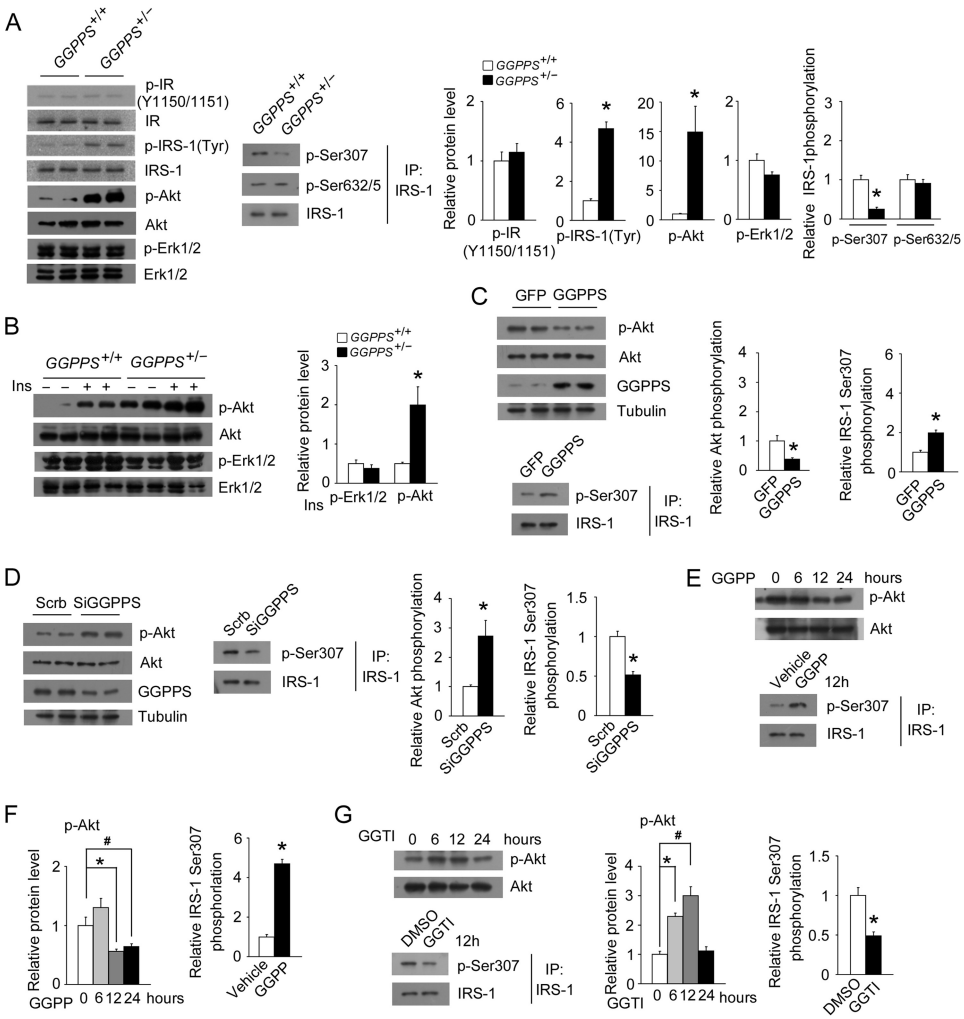

FIGURE 4. **Regulation of muscle insulin signaling by GGPPS.** *A*, protein expression in the gastrocnemius muscles of mice at 8 weeks of age ($n = 5$). *B*, insulin-stimulated Erk1/2 and Akt phosphorylation in the gastrocnemius muscles of mice at 8 weeks of age ($n = 5$). *C*, immunoblot analysis of Akt and IRS-1 (Ser-307) phosphorylation in L6 myotubes infected with the GFP or GGPPS adenovirus for 48 h. *D*, Akt and IRS-1 (Ser-307) phosphorylation in L6 myotubes transfected with Scrb or GGPPS siRNA for 48 h. *E–G*, Akt and IRS-1 (Ser-307) phosphorylation in L6 myotubes after GGPP (20 μM) or GGTI administration (20 μM) for the indicated time points. The data are shown with means ± S.D. * and #, $p < 0.05$. *Ins*, insulin; *IP*, immunoprecipitation.

that glucose uptake was controlled in a GGPPS-regulated protein geranylgeranylation-dependent manner (Fig. 7*D*). Next, we also assessed the RhoA prenylation and insulin signaling in a palmitate treatment model. Palmitate treatment also enhanced the prenylation of RhoA and phosphorylation of IRS-1 (Ser-307) in the L6 myotubes, whereas GGPPS knockdown or GGTI treatment was able to prevent this process (Fig. 7, *E* and *F*). Similarly, GGPPS knockdown or GGTI treatment notably reversed the reduction of Akt phosphorylation caused by palmitate incubation in the L6 myotubes (Fig. 7*G*). Thus, these results further confirm that GGPPS contributes to lipid-induced muscle insulin resistance.

Discussion

Increased circulating FFAs are a clinical characteristic of type 2 diabetes that has been implicated in the development of peripheral insulin resistance (22, 23). Skeletal muscle insulin resistance is a typical characteristic of patients with type 2 diabetes mellitus. Elevated FFA levels impair insulin sensitivity in muscle cells and also contribute to muscle insulin resistance in type 2 diabetes (2). Here, we showed that FFAs were able to induce GGPPS expression, which was responsible for the reduction in muscle insulin sensitivity that occurred in the diabetic mice. The MCK-*GGPPS*$^{+/-}$ mice fed a chow diet or HFD displayed improved systemic glucose homeostasis and insulin sensitivity. Knockdown of GGPPS expression also increased insulin sensitivity in the muscle cells. Furthermore, GGPPS knockdown rescued palmitate-induced insulin resistance in these cells. These results demonstrate that GGPPS indeed promotes FFA-induced skeletal muscle insulin resistance.

RhoA is a member of the Rho family of small GTPases, which includes Rho, Rac, and Cdc42 and is considered to regulate cytoskeletal dynamics through the action of Rho kinase (24–26). This enzyme cycles between a GDP-bound inactive state and a GTP-bound active state. The GTP-bound form of RhoA is located at the membrane, where it associates with downstream targets (24–26). RhoA is geranylgeranylated by isoprenoid lipids via geranylgeranyltransferase I, which catalyzes the covalent attachment of the geranylgeranyl group to the CAA*X* motif of RhoA (27). This is also important for the localization of

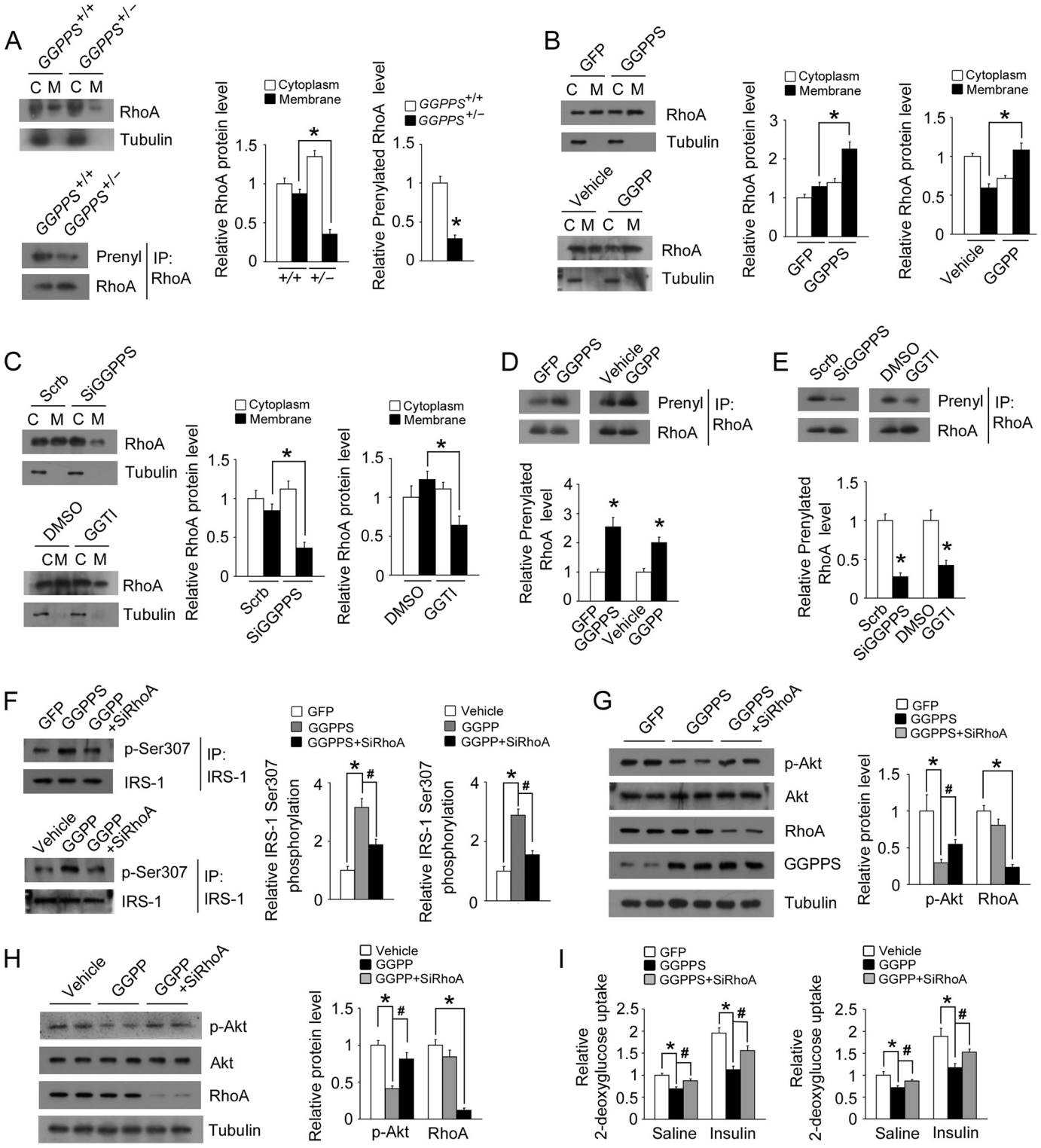

FIGURE 5. **RhoA geranylgeranylation mediates the regulation of insulin signaling by GGPPS.** *A*, the membrane association and prenylation of RhoA in the gastrocnemius muscles of WT and MCK-*GGPPS*$^{+/-}$ mice. *B*, the membrane association of RhoA in L6 myotubes after infection with the GFP or GGPPS adenovirus for 48 h or GGPP administration (20 μM) for 12 h. *C*, the membrane association of RhoA in L6 myotubes after transfection with Scrb or GGPPS siRNA for 48 h or GGTI administration (20 μM) for 12 h. *D*, the prenylation of RhoA in L6 myotubes after infection with the GFP or GGPPS adenovirus for 48 h or GGPP administration (20 μM) for 12 h. *E*, the prenylation of RhoA in L6 myotubes after transfection with Scrb or GGPPS siRNA for 48 h or GGTI administration (20 μM) for 12 h. *F*, the phosphorylation of IRS-1 (Ser-307) in L6 myotubes infected with the GGPPS adenovirus for 48 h after transfection with Scrb or RhoA siRNA for 6 h or the phosphorylation of IRS-1 (Ser-307) in L6 myotubes treated with GGPP (20 μM) for 12 h after transfection with RhoA siRNA for 40 h. *G*, protein expression in L6 myotubes infected with the GGPPS adenovirus for 48 h after transfection with Scrb or RhoA siRNA for 6 h. *H*, protein expression in L6 myotubes treated with GGPP (20 μM) for 12 h after transfection with Scrb or RhoA siRNA for 40 h. *I*, glucose uptake in L6 myotubes infected with the GGPPS adenovirus for 48 h after transfection with Scrb or RhoA siRNA for 6 h; glucose uptake in L6 myotubes treated with GGPP (20 μM) for 12 h after transfection with Scrb or RhoA siRNA for 40 h. The data represent means ± S.D. * and #, $p < 0.05$. *C*, cytoplasm; *M*, membrane; *IP*, immunoprecipitation.

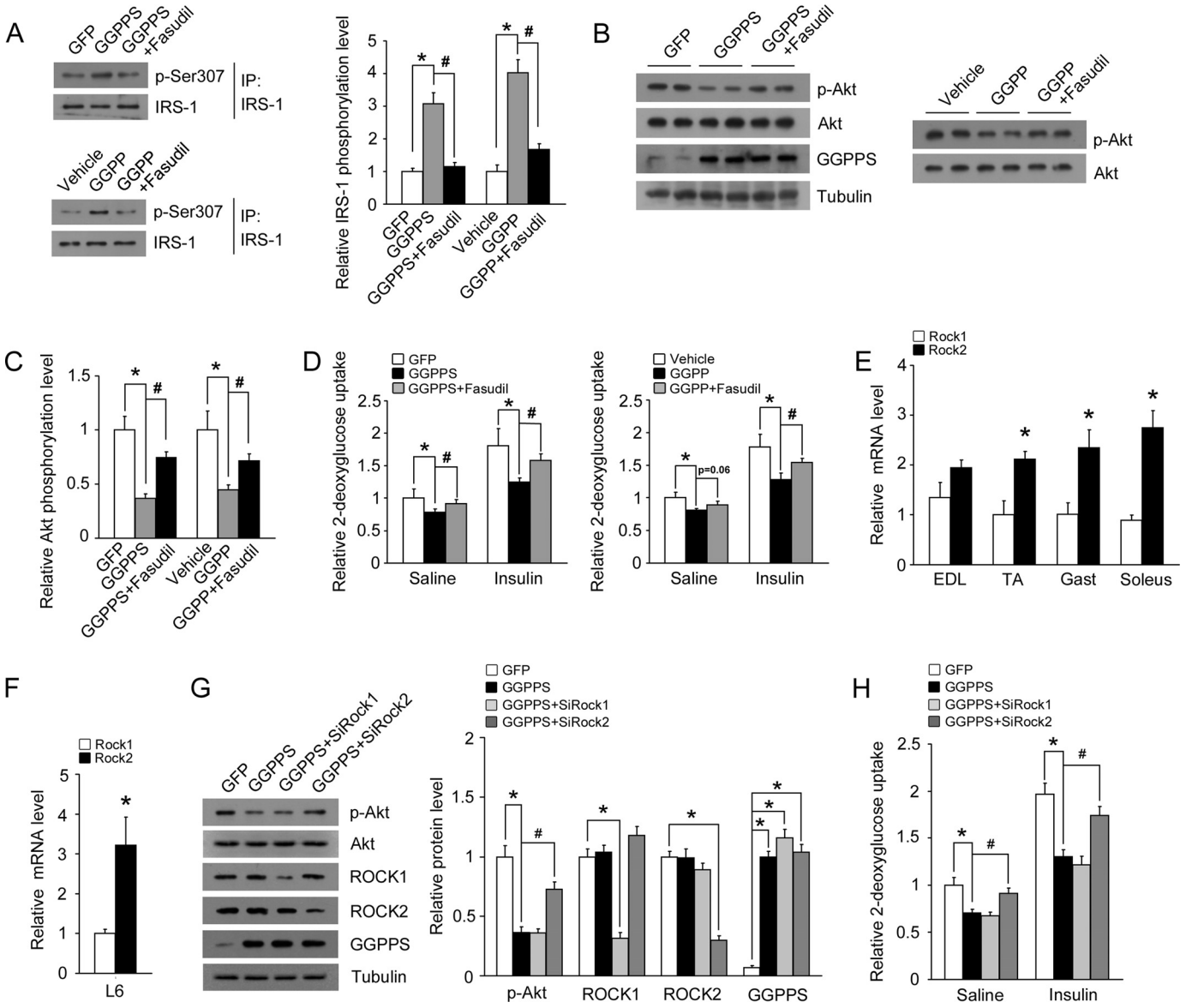

FIGURE 6. **Rho kinase inhibitor prevents inhibition of insulin signaling by GGPPS.** *A*, the phosphorylation of IRS-1 (Ser-307) in L6 myotubes treated with fasudil (10 μM) for 6 h after infection with the GGPPS adenovirus for 42 h or the phosphorylation of IRS-1 (Ser-307) in L6 myotubes treated with fasudil (10 μM) for 6 h after administration of GGPP (20 μM) for 6 h. *B* and *C*, immunoblot analysis of Akt phosphorylation in L6 myotubes treated with fasudil (10 μM) for 6 h after infection with the GGPPS adenovirus for 42 h or Akt phosphorylation in L6 myotubes treated with fasudil (10 μM) for 6 h after administration of GGPP (20 μM) for 6 h. *D*, glucose uptake in L6 myotubes treated with fasudil (10 μM) for 6 h after infection with the GGPPS adenovirus for 42 h. Glucose uptake in L6 myotubes treated with fasudil (10 μM) for 6 h after administration of GGPP (20 μM) for 6 h. *E*, qRT-PCR analysis of *Rock1* and *Rock2* mRNA expression in multiple muscle tissues. *F*, qRT-PCR analysis of *Rock1* and *Rock2* mRNA expression in L6 myotubes. *G*, protein expression in L6 myotubes infected with the GGPPS adenovirus for 48 h after transfection with Rock1 or Rock2 siRNA for 6 h. *H*, glucose uptake in L6 myotubes infected with the GGPPS adenovirus for 48 h after transfection with Rock1 or Rock2 siRNA for 6 h. The data are shown with means ± S.D. * and #, $p < 0.05$. *EDL*, extensor digitorum longus; *IP*, immunoprecipitation; *TA*, tibialis anterior.

the protein to the cellular membrane and the activation of downstream signaling. The RhoA/Rho kinase pathway plays an important role in the regulation of insulin resistance. Rho kinase has been reported to modulate insulin signaling by binding to IRS-1 and enhancing phosphorylation at serines 307 and 632/635 (18–21). A Rho kinase inhibitor, fasudil, also prevents lipid-induced insulin resistance and diabetes (20, 28). In skeletal muscle, the activated RhoA/Rho kinase signaling under obese and insulin-resistant conditions impairs insulin pathway through phosphorylation of the IRS-1 serine 307 residue, leading to the development of insulin resistance (20). Consistent with the aforementioned studies, our findings also showed that GGPPS-controlled protein geranylgeranylation could induce IRS-1 (Ser-307) phosphorylation through the RhoA/Rho kinase pathway, thereby promoting lipid-induced insulin resistance. Whether other factors or signaling pathways mediate the regulation of insulin signaling by GGPPS requires further investigation.

Kim and co-workers (29, 30) have reported that inhibition of the Rho kinase isoform Rock1 causes insulin resistance in skeletal muscle via inhibitory phosphorylation of IRS-1 and decreases downstream signaling, whereas Bankar's study (31) finds that heterozygous Rock2 deficiency augments skeletal muscle IRS-1/PI3K/Akt signaling and whole body insulin sen-

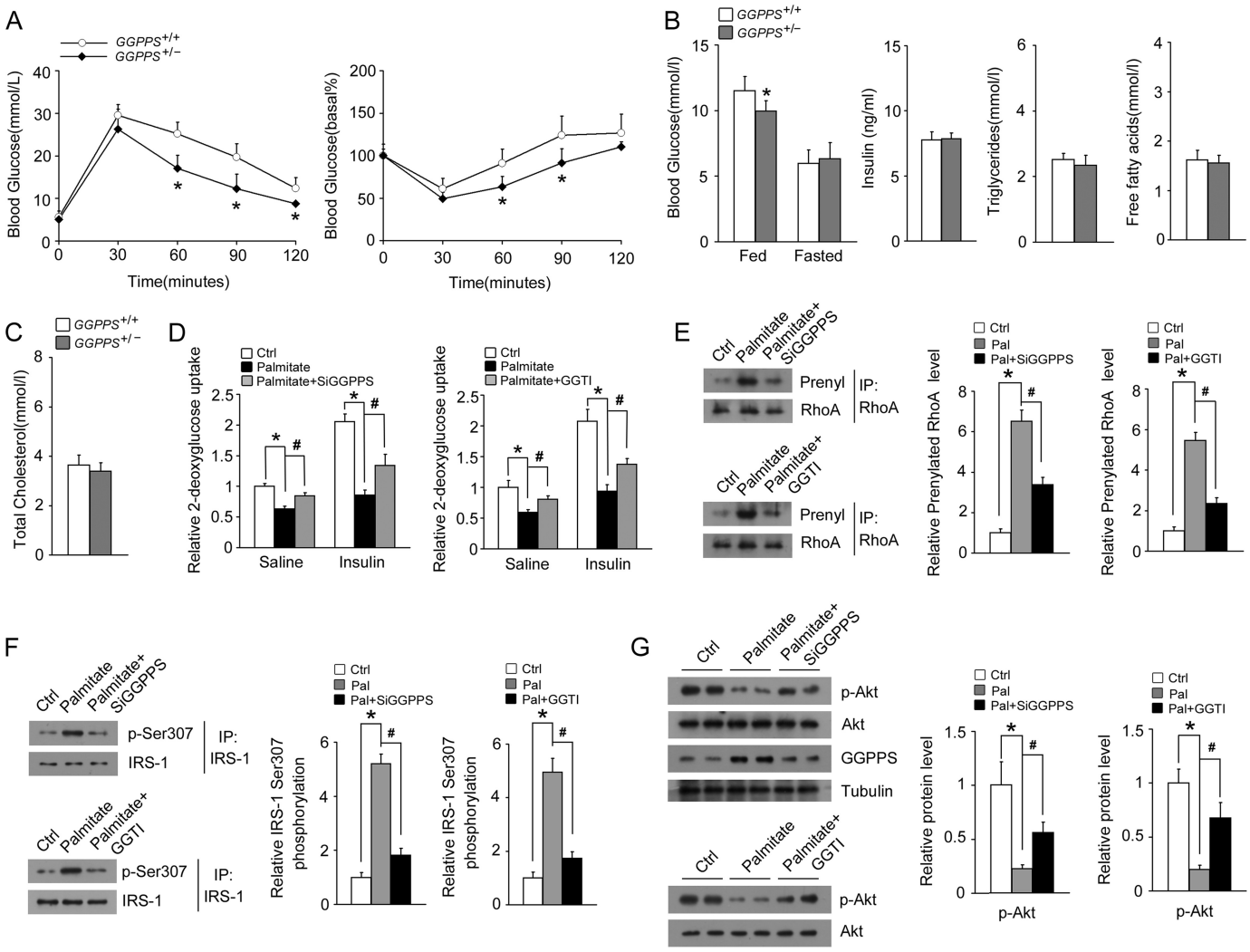

FIGURE 7. **Improved insulin sensitivity in MCK-*GGPPS*$^{+/-}$ mice fed a HFD.** *A–C*, GTTs, ITTs, blood glucose, fed insulin, fasted triglycerides, fasted FFAs, and fasted cholesterol levels in mice fed a HFD for 12 weeks ($n \geq 5$). *D*, glucose uptake in L6 myotubes incubated with 0.75 mM palmitate for 16 h after transfection with Scrb or GGPPS siRNA for 40 h; glucose uptake in L6 myotubes incubated with palmitate (0.75 mM) and GGTI (20 μM) for 16 h. *E*, the prenylation of RhoA in L6 myotubes incubated with 0.75 mM palmitate for 16 h after transfection with GGPPS siRNA for 40 h or the prenylation of RhoA in L6 myotubes incubated with 0.75 mM palmitate and 20 μM GGTI for 16 h. *F*, the phosphorylation of IRS-1 (Ser-307) in L6 myotubes incubated with 0.75 mM palmitate for 16 h after transfection with the GGPPS siRNA for 40 h or the phosphorylation of IRS-1 (Ser-307) in L6 myotubes incubated with 0.75 mM palmitate and 20 μM GGTI for 16 h. *G*, immunoblot analysis of Akt phosphorylation in L6 myotubes incubated with 0.75 mM palmitate for 16 h after transfection with GGPPS siRNA for 40 h or Akt phosphorylation in L6 myotubes incubated with palmitate (0.75 mM) and GGTI (20 μM) for 16 h. The data are shown with means ± S.D. * and #, $p < 0.05$. *Ctrl*, control; *IP*, immunoprecipitation; *Pal*, palmitate.

sitivity. These studies indicate that the role of Rock2 in regulation of insulin sensitivity is opposite to that of Rock1. Our study showed that skeletal muscle tissues have more abundant mRNA expression of *Rock2* than that of *Rock1,* which was consistent with previous report (32). These bring concerns to our findings suggesting that Rock2 may mainly mediate the GGPPS/RhoA signaling to regulate insulin pathway. Indeed, our results showed that Rock2, but not Rock1, mediates the GGPPS-regulated PI3K/Akt pathway and glucose transport in muscle cells. Because Rock1 and Rock2 display different expression patterns in various tissues (32), they may mainly function in their specific tissues. In skeletal muscle, Rock2 is the predominant Rho kinase isoform, so the effects of Rock1 may be masked by Rock2. Therefore, our findings demonstrate that Rock2 plays an important role in mediating upstream GGPPS/RhoA signaling in skeletal muscle.

The mevalonate pathway, which is responsible for cholesterol synthesis, is associated with insulin resistance and type 2 diabetes. An imbalance in plasma membrane cholesterol levels may induce obesity and insulin resistance in HFD-fed mice as well as obese human subjects (33). Although statins were reported to increase the incidence of diabetes, some studies have shown that statins might have improved effects on insulin resistance in mice and humans (34–37). Statin treatment prevents HFD-induced peripheral insulin resistance by increasing the IRS-1/PI3K/Akt pathway in the liver and muscle (38). In addition to inhibiting cholesterol synthesis, statins also reduce the synthesis of downstream intermediates of the mevalonate pathway, including farnesyl pyrophosphate and GGPP (39). Thus, they may decrease lipid-induced muscle insulin resistance by reducing the synthesis of GGPP.

In the present study, we did not find any alterations in muscle properties in the muscle-specific *GGPPS* knock-out mice, suggesting that deficiency of GGPP alone may not affect muscle morphology and performance. Statins can cause a variety of dose-dependent side effects, such as muscle pain, muscle cell damage, and severe rhabdomyolysis (40). Recently, Gee *et al.* (41) found that inhibition of prenyltransferase activity by statins in both liver and muscle cell lines is not causative of cytotoxicity. Thus, decreasing the activity of GGPPS or the RhoA/Rho kinase signaling but not HMG-CoA reductase of the mevalonate pathway may be a suitable strategy for the treatment of insulin resistance.

In conclusion, we have identified GGPPS, which is an important branch point enzyme in the mevalonate pathway that plays an important role in the promotion of lipid-induced insulin resistance in skeletal muscle. Our findings suggest that decreasing GGPPS activity in skeletal muscle may represent a new therapeutic target for the amelioration of insulin resistance and type 2 diabetes.

Author Contributions—W. T., B. X., and C.-J. L. designed research. W. T., J. W., B.-X. X, Y.-Y. Z., N. S., SJ, X. X. W., N. X., and C. J. performed research. S. C., X. G., and B. X. reviewed and edited the manuscript. W. T. and C. J. L. analyzed data. W. T. and C.-J. L. wrote the paper. All authors reviewed the results and approved the final version of the manuscript.

Acknowledgments—We thank Dr. Lei Cao and Prof. Gang Hu (Nanjing Medical University, Nanjing, China) for excellent technical assistance in rotarod test. We also thank Dr. Amira Klip (Hospital for Sick Children, Toronto, Canada) for providing L6 cells overexpressing c-MYC-GLUT4.

References

1. Guilherme, A., Virbasius, J. V., Puri, V., and Czech, M. P. (2008) Adipocyte dysfunctions linking obesity to insulin resistance and type 2 diabetes. *Nat. Rev. Mol. Cell Biol.* **9,** 367–377
2. Krssak, M., Falk Petersen, K., Dresner, A., DiPietro, L., Vogel, S. M., Rothman, D. L., Roden, M., and Shulman, G. I. (1999) Intramyocellular lipid concentrations are correlated with insulin sensitivity in humans: a ^{1}H NMR spectroscopy study. *Diabetologia* **42,** 113–116
3. Griffin, M. E., Marcucci, M. J., Cline, G. W., Bell, K., Barucci, N., Lee, D., Goodyear, L. J., Kraegen, E. W., White, M. F., and Shulman, G. I. (1999) Free fatty acid-induced insulin resistance is associated with activation of protein kinase C theta and alterations in the insulin signaling cascade. *Diabetes* **48,** 1270–1274
4. Savage, D. B., Petersen, K. F., and Shulman, G. I. (2007) Disordered lipid metabolism and the pathogenesis of insulin resistance. *Physiol. Rev.* **87,** 507–520
5. Kraegen, E. W., and Cooney, G. J. (2008) Free fatty acids and skeletal muscle insulin resistance. *Curr. Opin. Lipidol.* **19,** 235–241
6. Zhang, F. L., and Casey, P. J. (1996) Protein prenylation: molecular mechanisms and functional consequences. *Annu. Rev. Biochem.* **65,** 241–269
7. Xu, N., Guan, S., Chen, Z., Yu, Y., Xie, J., Pan, F. Y., Zhao, N. W., Liu, L., Yang, Z. Z., Gao, X., Xu, B., and Li, C. J. (2015) The alteration of protein prenylation induces cardiomyocyte hypertrophy through Rheb-mTORC1 signalling and leads to chronic heart failure. *J. Pathol.* **235,** 672–685
8. Wang, X. X., Ying, P., Diao, F., Wang, Q., Ye, D., Jiang, C., Shen, N., Xu, N., Chen, W. B., Lai, S. S., Jiang, S., Miao, X. L., Feng, J., Tao, W. W., Zhao, N. W., Yao, B., Xu, Z. P., Sun, H. X., Li, J. M., Sha, J. H., Huang, X. X., Shi, Q. H., Tang, H., Gao, X., and Li, C. J. (2013) Altered protein prenylation in Sertoli cells is associated with adult infertility resulting from childhood mumps infection. *J. Exp. Med.* **210,** 1559–1574
9. Shen, N., Gong, T., Wang, J. D., Meng, F. L., Qiao, L., Yang, R. L., Xue, B., Pan, F. Y., Zhou, X. J., Chen, H. Q., Ning, W., and Li, C. J. (2011) Cigarette smoke-induced pulmonary inflammatory responses are mediated by EGR-1/GGPPS/MAPK signaling. *Am. J. Pathol.* **178,** 110–118
10. Weivoda, M. M., and Hohl, R. J. (2012) Geranylgeranyl pyrophosphate stimulates PPARγ expression and adipogenesis through the inhibition of osteoblast differentiation. *Bone* **50,** 467–476
11. Shen, N., Yu, X., Pan, F.-Y., Gao, X., Xue, B., and Li, C.-J. (2011) An early response transcription factor, Egr-1, enhances insulin resistance in type 2 diabetes with chronic hyperinsulinism. *J. Biol. Chem.* **286,** 14508–14515
12. Yu, X., Shen, N., Zhang, M. L., Pan, F. Y., Wang, C., Jia, W. P., Liu, C., Gao, Q., Gao, X., Xue, B., and Li, C. J. (2011) Egr-1 decreases adipocyte insulin sensitivity by tilting PI3K/Akt and MAPK signal balance in mice. *EMBO J.* **30,** 3754–3765
13. Vicent, D., Maratos-Flier, E., and Kahn, C. R. (2000) The branch point enzyme of the mevalonate pathway for protein prenylation is overexpressed in the ob/ob mouse and induced by adipogenesis. *Mol. Cell. Biol.* **20,** 2158–2166
14. Blonder, J., Chan, K. C., Issaq, H. J., and Veenstra, T. D. (2006) Identification of membrane proteins from mammalian cell/tissue using methanol-facilitated solubilization and tryptic digestion coupled with 2D-LC-MS/MS. *Nat. Protoc.* **1,** 2784–2790
15. Moyers, J. S., Bilan, P. J., Reynet, C., and Kahn, C. R. (1996) Overexpression of Rad inhibits glucose uptake in cultured muscle and fat cells. *J. Biol. Chem.* **271,** 23111–23116
16. Chen, S., Wasserman, D. H., MacKintosh, C., and Sakamoto, K. (2011) Mice with AS160/TBC1D4-Thr649Ala knockin mutation are glucose intolerant with reduced insulin sensitivity and altered GLUT4 trafficking. *Cell Metab.* **13,** 68–79
17. Sakamoto, K., McCarthy, A., Smith, D., Green, K. A., Grahame Hardie, D., Ashworth, A., and Alessi, D. R. (2005) Deficiency of LKB1 in skeletal muscle prevents AMPK activation and glucose uptake during contraction. *EMBO J.* **24,** 1810–1820
18. Farah, S., Agazie, Y., Ohan, N., Ngsee, J. K., and Liu, X. J. (1998) A Rho-associated protein kinase, ROKα, binds insulin receptor substrate-1 and modulates insulin signaling. *J. Biol. Chem.* **273,** 4740–4746
19. Begum, N., Sandu, O. A., Ito, M., Lohmann, S. M., and Smolenski, A. (2002) Active Rho kinase (ROK-α) associates with insulin receptor substrate-1 and inhibits insulin signaling in vascular smooth muscle cells. *J. Biol. Chem.* **277,** 6214–6222
20. Kanda, T., Wakino, S., Homma, K., Yoshioka, K., Tatematsu, S., Hasegawa, K., Takamatsu, I., Sugano, N., Hayashi, K., and Saruta, T. (2006) Rho-kinase as a molecular target for insulin resistance and hypertension. *FASEB J.* **20,** 169–171
21. Lim, M. J., Choi, K. J., Ding, Y., Kim, J. H., Kim, B. S., Kim, Y. H., Lee, J., Choe, W., Kang, I., Ha, J., Yoon, K. S., and Kim, S. S. (2007) RhoA/Rho kinase blocks muscle differentiation via serine phosphorylation of insulin receptor substrate-1 and -2. *Mol. Endocrinol.* **21,** 2282–2293
22. Senn, J. J. (2006) Toll-like receptor-2 is essential for the development of palmitate-induced insulin resistance in myotubes. *J. Biol. Chem.* **281,** 26865–26875
23. Thrush, A. B., Heigenhauser, G. J., Mullen, K. L., Wright, D. C., and Dyck, D. J. (2008) Palmitate acutely induces insulin resistance in isolated muscle from obese but not lean humans. *Am. J. Physiol. Regul. Integr. Comp. Physiol.* **294,** R1205–R1212
24. Hall, A. (1998) Rho GTPases and the actin cytoskeleton. *Science* **279,** 509–514
25. Ridley, A. J., and Hall, A. (1992) The small GTP-binding protein rho regulates the assembly of focal adhesions and actin stress fibers in response to growth factors. *Cell* **70,** 389–399
26. Ridley, A. J., Paterson, H. F., Johnston, C. L., Diekmann, D., and Hall, A. (1992) The small GTP-binding protein rac regulates growth factor-induced membrane ruffling. *Cell* **70,** 401–410
27. Moores, S. L., Schaber, M. D., Mosser, S. D., Rands, E., O'Hara, M. B., Garsky, V. M., Marshall, M. S., Pompliano, D. L., and Gibbs, J. B. (1991) Sequence dependence of protein isoprenylation. *J. Biol. Chem.* **266,** 14603–14610

28. Kikuchi, Y., Yamada, M., Imakiire, T., Kushiyama, T., Higashi, K., Hyodo, N., Yamamoto, K., Oda, T., Suzuki, S., and Miura, S. (2007) A Rho-kinase inhibitor, fasudil, prevents development of diabetes and nephropathy in insulin-resistant diabetic rats. *J. Endocrinol.* **192,** 595–603
29. Lee, D. H., Shi, J., Jeoung, N. H., Kim, M. S., Zabolotny, J. M., Lee, S. W., White, M. F., Wei, L., and Kim, Y. B. (2009) Targeted disruption of ROCK1 causes insulin resistance *in vivo*. *J. Biol. Chem.* **284,** 11776–11780
30. Chun, K. H., Araki, K., Jee, Y., Lee, D. H., Oh, B. C., Huang, H., Park, K. S., Lee, S. W., Zabolotny, J. M., and Kim, Y. B. (2012) Regulation of glucose transport by ROCK1 differs from that of ROCK2 and is controlled by actin polymerization. *Endocrinology* **153,** 1649–1662
31. Bankar, G. (2013) Heterozygous Rho kinase 2 deficinecy increases whole body insulin sensitivity in mice, M.S. thesis, University of British Columbia
32. Pelosi, M., Marampon, F., Zani, B. M., Prudente, S., Perlas, E., Caputo, V., Cianetti, L., Berno, V., Narumiya, S., Kang, S. W., Musarò, A., and Rosenthal, N. (2007) ROCK2 and its alternatively spliced isoform ROCK2m positively control the maturation of the myogenic program. *Mol. Cell. Biol.* **27,** 6163–6176
33. Taghibiglou, C., Bradley, C. A., Gaertner, T., Li, Y., Wang, Y., and Wang, Y. T. (2009) Mechanisms involved in cholesterol-induced neuronal insulin resistance. *Neuropharmacology* **57,** 268–276
34. Suzuki, M., Kakuta, H., Takahashi, A., Shimano, H., Tada-Iida, K., Yokoo, T., Kihara, R., and Yamada, N. (2005) Effects of atorvastatin on glucose metabolism and insulin resistance in KK/Ay mice. *J. Atheroscler. Thromb.* **12,** 77–84
35. Okada, K., Maeda, N., Kikuchi, K., Tatsukawa, M., Sawayama, Y., and Hayashi, J. (2005) Pravastatin improves insulin resistance in dyslipidemic patients. *J. Atheroscler. Thromb.* **12,** 322–329
36. Huptas, S., Geiss, H. C., Otto, C., and Parhofer, K. G. (2006) Effect of atorvastatin (10 mg/day) on glucose metabolism in patients with the metabolic syndrome. *Am. J. Cardiol.* **98,** 66–69
37. Sattar, N., Preiss, D., Murray, H. M., Welsh, P., Buckley, B. M., de Craen, A. J., Seshasai, S. R., McMurray, J. J., Freeman, D. J., Jukema, J. W., Macfarlane, P. W., Packard, C. J., Stott, D. J., Westendorp, R. G., Shepherd, J., Davis, B. R., Pressel, S. L., Marchioli, R., Marfisi, R. M., Maggioni, A. P., Tavazzi, L., Tognoni, G., Kjekshus, J., Pedersen, T. R., Cook, T. J., Gotto, A. M., Clearfield, M. B., Downs, J. R., Nakamura, H., Ohashi, Y., Mizuno, K., Ray, K. K., and Ford, I. (2010) Statins and risk of incident diabetes: a collaborative meta-analysis of randomised statin trials. *Lancet* **375,** 735–742
38. Lalli, C. A., Pauli, J. R., Prada, P. O., Cintra, D. E., Ropelle, E. R., Velloso, L. A., and Saad, M. J. (2008) Statin modulates insulin signaling and insulin resistance in liver and muscle of rats fed a high-fat diet. *Metabolism* **57,** 57–65
39. Goldstein, J. L., and Brown, M. S. (1990) Regulation of the mevalonate pathway. *Nature* **343,** 425–430
40. Thompson, P. D., Clarkson, P., and Karas, R. H. (2003) Statin-associated myopathy. *JAMA* **289,** 1681–1690
41. Gee, R. H., Spinks, J. N., Malia, J. M., Johnston, J. D., Plant, N. J., and Plant, K. E. (2015) Inhibition of prenyltransferase activity by statins in both liver and muscle cell lines is not causative of cytotoxicity. *Toxicology* **329,** 40–48